

Cyclooxygenase-2 Influences Response to Co-Targeting of MEK and CDK4/6 in a Subpopulation of Pancreatic Cancers

Joel D. Maust¹, Christy L. Frankowski-McGregor², Armand Bankhead III^{3,4}, Diane M. Simeone^{5*},
Judith S. Sebolt-Leopold^{1,2}

¹Department of Pharmacology, University of Michigan Medical School, Ann Arbor MI.

²Department of Radiology, University of Michigan Medical School, Ann Arbor MI.

³Department of Biostatistics, University of Michigan School of Public Health, Ann Arbor, MI

⁴Department of Computational Medicine and Bioinformatics, University of Michigan Medical School, Ann Arbor MI.

⁵Department of Surgery, University of Michigan Medical School, Ann Arbor MI.

*Current affiliation:

Department of Surgery, Department of Pathology, NYU Langone Medical Center, New York NY.

Running title: Co-targeting of MEK and CDK4/6 to treat pancreatic cancer

Keywords: MEK, CDK4/6, COX-2, pancreatic cancer.

Financial Support: This research was funded by NIH R01CA155198 (J.S. Leopold), P50CA130810 (J.S. Leopold), T32-GM007767 (J.D. Maust), and Luchessi Fellowship (J.D. Maust). Research reported in this publication was further supported by the National Cancer Institute of the National Institutes of Health under award number P30CA046592.

Correspondence:

Judith Sebolt-Leopold, Ph.D.
Research Professor, Departments of Radiology and Pharmacology
University of Michigan Medical School
NCRC B520-1365, 1600 Huron Pkwy, Ann Arbor, MI
T: (734) 615-7326, jssl@med.umich.edu

Disclosure of conflict of interest: The authors declare no potential conflicts of interest.

Abstract

The ineffectiveness of chemotherapy in patients with pancreatic cancer highlights a critical unmet need in pancreatic cancer therapy. Two commonly mutated genes in pancreatic cancer, KRAS and CDKN2A, have an incidence exceeding 90%, supporting investigation of dual targeting of MEK and CDK4/6 as a potential therapeutic strategy for this patient population. An *in vitro* proliferation synergy screen was conducted to evaluate response of a panel of high passage and patient-derived pancreatic cancer models to the combination of trametinib and palbociclib to inhibit MEK and CDK4/6, respectively. Two adenosquamous carcinoma models, L3.6pl and UM59, stood out for their high synergy response. *In vivo* studies confirmed that this combination treatment approach was highly effective in subcutaneously implanted L3.6pl and UM59 tumor-bearing animals. Both models were refractory to single agent treatment. Reverse phase protein array analysis of L3.6pl tumors excised from treated animals revealed strong down regulation of cyclooxygenase-2 (COX-2) expression in response to combination treatment. Expression of COX-2 under a CMV-driven promoter and shRNA knockdown of COX-2 both led to resistance to combination treatment. Our findings suggest that COX-2 may be involved in the improved therapeutic outcome seen in some pancreatic tumors that fail to respond to MEK or CDK4/6 inhibitors alone but respond favorably to their combination.

Introduction

Pancreatic cancer is the third leading cause of cancer-related deaths in the US and has the lowest 5-year relative survival rate of any cancer (1,2). This disease is recalcitrant to chemotherapeutic approaches and recently approved therapies afford only modest improvements in survival. Consequently, the 5-year survival rate since the 1970's has only improved from 3% to 8% (2). There exists a critical unmet need for development of novel treatments for patients diagnosed with this disease.

The most commonly mutated genes in pancreatic cancer are KRAS, which occurs in over 90% of tumors, and CDKN2A (inactivated in >90% of cases), the gene encoding the endogenous CDK4/6 inhibitor p16^{INK4a} (3-6). KRAS is a small GTPase that activates the mitogen activated protein kinase (MAPK) signaling pathway, whereas p16 is a potent suppressor of oncogenic transformation and a key mediator of RAS induced senescence (7). While MEK inhibitors have exhibited potent *in vitro* activity in KRAS mutant tumor cells (8), the *in vivo* activity of these agents has been disappointing due to the development of resistance (8-11).

An attractive target for MEK inhibitor-based combinations is CDK4/6, a kinase crucial for the transition from G1 to S phase (12). In support of co-targeting MEK and CDK4/6, a synthetic lethal interaction between KRAS and CDK4 was found in non-small cell lung cancer (13). Furthermore, CDK4 was identified as a key driver of an alternative phenotype induced by MEK inhibition, but not genetic extinction of NRAS in mouse models of melanoma (14). Our laboratory as well as Kopetz and colleagues subsequently demonstrated *in vivo* efficacy of this combination approach in KRAS mutant patient-derived xenograft (PDX) models of colorectal cancer (15,16). Pancreatic cancers should also derive therapeutic benefit from this combination strategy based on their genomic features. Specifically, activating KRAS mutations have been shown to initiate formation of premalignant lesions in mouse models of pancreatic cancer, while loss of p16 has been shown to enable their malignant progression (17). Ectopic p16 expression can induce senescence and apoptosis when reintroduced into pancreatic cancer cell lines with CDKN2A deletions (18). Since CDK4 and CDK6 are the sole targets of p16, a unique opportunity is present to leverage recently approved CDK4/6 inhibitors to recapitulate this phenotype in pancreatic cancer.

The effectiveness of dual targeting of MEK and CDK4/6 to treat pancreatic cancer has been reported for high passage models (19,20). The present report extends these findings to include patient

derived xenograft (PDX) models of pancreatic cancer and concurrent phosphoproteomic profiling to identify potential prognostic biomarkers of response. We report here that two adenosquamous pancreatic models are highly responsive to dual targeting of these kinases both *in vitro* and *in vivo*. We further find that genetic manipulation of cyclooxygenase-2 (COX-2) expression, which is highly expressed in both of these models, blunts therapeutic effectiveness of combination treatment. Our results therefore provide the impetus to further explore the prognostic role of COX-2 to aid in the identification of a subpopulation of pancreatic cancer patients who might derive the greatest therapeutic benefit from combination therapy directed against MEK and CDK4/6.

Materials and Methods

Chemicals

Trametinib and binimetinib (MEK162) were purchased from LC Laboratories. Ribociclib (LEE011) was purchased from Chemietek. Palbociclib isethionate was purchased from Selleckchem. Drug stocks were dissolved in DMSO at 10 mM and stored at -20 °C.

Cell proliferation assays

For growth inhibition and synergy analyses, cells were seeded in white-walled/clear bottom tissue culture treated 96-well plates at 5,000-10,000 cells/well and allowed to adhere for 24 hours followed by addition of growth media containing serial dilutions of trametinib, palbociclib, or both drugs in combination. Cells were incubated for 5 days in the continuous presence of drug or DMSO and viability was measured using CellTiter-Glo (Promega). Viability was calculated as a percentage of DMSO treated cells. Concentration response curves were modeled using a nonlinear regression curve fit with a sigmoidal concentration response using GraphPad Prism 6. Synergy plot calculations were performed using Combenefit software (Cancer Research UK Cambridge Institute) and scores were

generated using Chalice Bioinformatics Software (Horizon Discovery Group), both using the Loewe model of synergy.

Cell lines

All cell lines were cultured at 37°C in 5% CO₂ in 10% FBS and 1% penicillin/streptomycin (Thermo Fisher Scientific). L3.6pl, pL45, MiaPaCa-2, Panc-1 and HS766T cell lines were grown in DMEM. HPAFII was grown in EMEM. ASPC1, Bxpc-3 and Panc10.05 were cultured in RPMI media. The PDX models UM8, UM15, UM16, UM19, UM32, UM53, UM59, UM81, UM90, UM91 and UM123 were established to grow in animals and in culture. All PDX models originated from patients providing informed written consent and undergoing surgical resection at University of Michigan. All patient samples were procured with approval of the University of Michigan Institutional Review Board. All PDX lines were grown in RPMI media. All lines were negative for mycoplasma contamination when tested with MycoAlert Mycoplasma Detection Kit (Lonza). All high passage cell lines were authenticated by short tandem repeat (STR) profiling at the University of Michigan Sequencing Core.

Cell cycle analysis

Cells were seeded into 6 well plates at ~150,000 cells/well and treated the next day at the indicated concentrations, with a maximum DMSO concentration of 0.1%. Cells were harvested with 0.05% trypsin, washed twice with PBS and fixed with 70% ethanol at 4°C for at least 24 hr. Cells were washed twice with PBS and incubated for 30 minutes in a solution of 50 µg/ml propidium iodide (Life Technologies, P3566), 0.1% Triton X- 100 (Sigma-Aldrich, T9284), 50 µg/ml RNase A (Qiagen, 1007885) and PBS. Data were collected on a Cyan ADP Analyzer (Beckman Coulter), with collection of at least 10,000 events. The analysis was performed using flow cytometry analysis software ModFit LT V4.0.5 (Verity Software House).

Animal studies

All procedures related to the handling, care, and treatment of animals were conducted in accordance with University of Michigan's Committee on the Use and Care of Animals guidelines. Cells (1×10^6) were injected subcutaneously into the region of the right axilla of 6- to 7-week-old female NCR nude mice (NCRNU-F sp/sp CrTac:NCr-*Foxn1*^{nu}, Taconic) in a 50:50 mixture of DMEM/F12 and Matrigel. Tumors were allowed to grow until 150-300 mm³, at which time mice were randomized into different treatment groups (4-5 animals per group). Trametinib and palbociclib were administered as a fine suspension in 0.5% HPMC with 0.2% Tween-80 or saline, respectively, based on individual animal body weight (0.2 ml/20 g), once daily via oral gavage. Tumor volumes were measured using calipers and calculated using the formula: tumor volume = (length*width²)/2. Efficacy was calculated as the ratio of change in mean tumor burdens at time t ($\Delta T/\Delta C$) where ΔT and ΔC is calculated as mean tumor burden at time t minus the mean tumor burden on the first day of treatment. Percent regression is calculated as $[-(\Delta T/T_0)*100]$, where T_0 is initial body weight of treated animals. Tumor growth delay was calculated based on the time required for the mean to reach ~750 mm³. Where applicable, statistical significance between groups was calculated on the last day of treatment via one-way ANOVA analysis with multiple comparisons between all treatment arms.

Western blotting and reverse-phase protein array (RPPA) analysis

Cells were harvested by scraping in the presence of radioimmunoprecipitation (RIPA) buffer plus phosphatase and protease inhibitors (Roche). Samples were denatured and normalized to 1 $\mu\text{g}/\mu\text{l}$ in LDS sample buffer (ThermoFisher) and 62.5 mM DTT (ThermoFisher). For immunoblotting, multiple independent immunoblots were used to present data from single experiments. Loading controls were probed on the same blot, with a representative image shown for experiments with multiple antibodies.

Ten micrograms of protein were run on precast 4-12% polyacrylamide gels (ThermoFisher). The following antibodies were used: pRb S780, pRb S807/11, Cdc6, total Rb, pERK, cyclin D1, COX-2, EGFR Y1068, FOXM1 (Cell Signaling), Pcd4 (Rockland), Beta-actin and GAPDH (Abcam). For RPPA analysis, tumors were homogenized and protein was extracted utilizing NP-40 lysis buffer plus phosphatase and protease inhibitors. Samples were denatured and normalized to 1 $\mu\text{g}/\mu\text{l}$ in SDS sample buffer/ β -mercaptoethanol (ThermoFisher) and shipped to the MD Anderson RPPA Core Facility, where samples were profiled and processed. Per the protein loading protocol, all antibodies were median centered per antibody, then median centered per sample, and log₂ normalized. Trametinib, palbociclib and combination treated samples were compared to control samples using a two-sample t-test for each treatment/control comparison. T-test p-values were adjusted for multiple testing using the FDR method and resulting qValues < 0.1 were considered to represent significant changes. Significant antibodies and treatment sample replicates are clustered using agglomerative hierarchical clustering with a Euclidean distance metric.

Immunohistochemistry

Tissues were fixed in 10% NBF, embedded in paraffin and sectioned according to standard procedures. The Ki67 antibody was obtained from Cell Signaling Technology. Representative images were obtained with a Nikon E-800 microscope, Olympus DP71 digital camera, and DP Controller software. To quantify the ratio of Ki67 positive nuclei to total nuclei, 5-8 snapshots of different sections of the tumor were used to determine the average Ki67 nuclear ratio using online software tool ImmunoRatio (21). Statistical significance was calculated between groups using one-way ANOVA (GraphPad Prism).

COX-2 plasmid construction and shRNA transduction

Full length human COX-2 cDNA was excised as a BamHI/XhoI fragment from the huCOX-2 pcDNA5/FRT/TO construct, generously provided by Dr. William Smith (University of Michigan, Ann Arbor, MI), and ligated into pcDNA3.1. Transfections of L3.6pl cells were performed in six-well dishes using huCOX-2 pcDNA3.1 linearized with Bgl II (2.5 µg plasmid/well) and Lipofectamine 2000 (ThermoFisher) according to manufacturer's instructions. Clones stably expressing full length human COX-2 were established after selection in medium containing 1 mg/mL G418 (ThermoFisher). Control (sc-108080) and COX-2 (sc-29279-V) shRNA lentiviral particles (Santa Cruz Biotechnology) were transduced into cells according to manufacturer's directions and clones were established after selection with 10 µg/ml puromycin.

Reverse-transcription quantitative PCR (RT-qPCR)

Total RNA was isolated from cell lines treated for 5 days using the RNeasy Mini Kit (Qiagen). First-strand cDNA was reverse-transcribed from total RNA using the SuperScript III First-Strand Synthesis System (Invitrogen) according to the manufacturer's instructions. Quantitative targeted amplification of cDNAs was performed using Taqman Gene Expression Assays primer/probe sets for COX-2 (Hs00153133_m1), Pcd4 (Hs00377253_m1), GAPDH (Hs02786624_g1) and Fast Advanced Master Mix (Thermo Fisher) according to the manufacturer's instructions. GAPDH was used as an endogenous control. The amplification conditions for the ViiA 7 Real-Time PCR System (Applied Biosystems) consisted of an initial step of 2 min at 50°C and 10 min at 95°C followed by 40 cycles of 15 sec 95°C, 1 min 60°C. For treated cells, data were analyzed using the $\Delta\Delta C_t$ method and expressed as fold change over control. Data from the panel of cell lines were calculated as one C_t equals a 2-fold difference in expression and are represented as relative expression to the highest expressing cell line.

Results

Inhibitors of MEK and CDK4/6 synergistically inhibit pancreatic cancer cell line growth

Screening of high passage and PDX models of pancreatic cancer was carried out to identify models in which the combined action of trametinib and palbociclib showed the greatest degree of synergy. Cell lines showed a wide range of response to combination treatment, as depicted in Figure 1A where models are listed in the order of a consolidated synergy score. L3.6pl cells showed the highest degree of synergy followed by UM59 cells, with both models exhibiting at least a two-fold increase over the panel median (2.35) (Fig. 1B). Synergistic response was greatest in response to the combination of trametinib and palbociclib at concentrations of 10 nM and 1 μ M, respectively, concentrations which led to a median reduction in viability of 59% across the panel (Supplementary Fig. S1A). These optimal concentrations are consistent with our previous work in colorectal cancer models (15) as well as the studies of others carried out in lung cancer models (22). A similar degree of synergy was observed when L3.6pl cells were treated with the MEK inhibitor binimetinib (23) and the CDK4/6 inhibitor ribociclib (24), confirming that synergy is not likely attributable to off target activities (Supplementary Fig. S1B). Comparative analysis of concentration response curves for high (L3.6pl), intermediate (UM59) and low (Bxpc-3 and Panc10.05) synergy models is shown in Figure 1C to better understand the relationship between synergy and sensitivity. As shown here, the degree of synergy decreased as the concentration of trametinib was raised. No synergy was observed in Bxpc-3 and Panc10.05 cells at concentrations greater than approximately 20 nM, where the concentration response curves for trametinib single agent and the combination treatment plots intersect. In contrast, the concentration response curves for L3.6pl cells never intersected, since viability could not be reduced beyond 50% despite use of high (1-10 μ M) concentrations of trametinib. These cells are also refractory to palbociclib treatment alone (Supplementary Figure S2A).

Co-targeting MEK and CDK4/6 leads to profound G1 arrest

MEK and CDK4/6 have both been shown to play a role in controlling cell cycle progression, either through induction of cyclins or phosphorylation of Retinoblastoma protein (Rb), a master regulator of G1-S progression. Cell cycle studies carried out in the L3.6pl and UM59 models confirmed that combination treatment with trametinib and palbociclib induces a strong time-dependent G1 arrest at concentrations previously shown to be synergistic (Fig. 2A). Immunoblotting analysis further revealed that expression levels of Cdc6, a protein critical for initiation of DNA synthesis and pre-replication complex assembly (25,26), and phosphorylated Rb, were selectively reduced in L3.6pl cells treated with the combination, consistent with G1 arrest (Fig. 2B). These data suggest that synergy between trametinib and palbociclib to inhibit cell growth is driven at least in part by enhancement of G1 arrest.

Uncoupling of Cyclin D1 and pRB expression in response to MEK inhibition is cell line dependent

Immunoblotting analyses confirmed that phosphorylated ERK levels were suppressed by trametinib treatment in all lines at concentrations consistent with a reduction in viability (Fig. 3A & 3B). MEK inhibition additionally led to a reduction of total and phosphorylated Rb levels in a concentration-dependent manner. This result is not surprising, as MAPK signaling has been shown to contribute to control of cyclin D1 expression in response to growth factor stimulation (27), thereby indirectly reducing CDK4/6 phosphorylation of Rb. Cyclin D1 levels were recalcitrant to MEK inhibition in cell lines previously found to be most responsive to combination treatment (L3.6pl, UM59), despite reduction in pRb expression. This reduction in pRb can be explained by increased p27 expression in response to trametinib treatment (Supplementary Fig. S2B), which has been shown to bind and contribute to inhibition of the CDK4/cyclin D complex (28). In contrast, models showing a low degree of synergy (Panc10.05, Bxpc-3) exhibited significant reduction in levels of both cyclin D1 and pRb in response to trametinib single agent treatment. While UM59 may be as sensitive to trametinib as

Panc10.05 and Bxpc-3 (Fig. 3A), trametinib clearly shows cell line-dependent effects on expression of these cell cycle proteins, likely contributing to comparative differences in synergistic potential with palbociclib. Collectively, these data suggest that tumors exhibiting MEK-dependent uncoupling of cyclin D1 and pRb expression *in vitro* may be most sensitive to dual targeting of MEK and CDK4/6.

Combination treatment with trametinib and palbociclib provides therapeutic benefit *in vivo*

Based on the high degree of *in vitro* synergy seen when MEK and CDK4/6 are both inhibited in L3.6pl cells, we evaluated the *in vivo* efficacy of the combination of trametinib and palbociclib in L3.6pl tumor-bearing animals. Daily treatment was initiated when tumors were advanced ($\sim 300 \text{ mm}^3$) for a total of 7 days. No signs of toxicity were noted at the doses administered. Neither single agent elicited a meaningful effect on $\Delta T/\Delta C$ or tumor growth delay after cessation of treatment (Fig. 4A). In contrast, a $\Delta T/\Delta C$ of 28% and a tumor growth delay of 10 days was observed in the combination arm. Tumors were harvested on the last day of treatment for immunohistochemical analysis of Ki67 expression (Fig. 4B-C), revealing a significant reduction in expression in tumors from the combination group compared to the control and single agent groups. The results from this study were subsequently confirmed with less advanced L3.6pl tumors at treatment initiation, showing a $\Delta T/\Delta C$ of 1% and a 15 day growth delay, versus 1 & 2 days for trametinib and palbociclib, respectively (Supplementary Fig. S3).

COX-2 expression is downregulated and Pcd4 is upregulated in response to co-targeting of MEK and CDK4/6

L3.6pl tumors evaluated for *in vivo* efficacy were further analyzed for selective proteomic changes as a consequence of combination treatment. Two proteins, COX-2 and programmed cell death 4 (Pcd4), emerged from Reverse Phase Protein Array (RPPA) analyses showing inverse dysregulation in response to treatment with trametinib and palbociclib (Fig. 4D). COX-2 expression showed the highest magnitude of change in the combination arm among all the proteins measured in the RPPA

platform. Palbociclib treatment caused a small decrease in COX-2, but this change was not significant. Others have noted the role of palbociclib in mediating a c-jun-dependent decrease in COX-2 expression, but the impact of this change outside of the epithelial-mesenchymal transition is unclear (29). An induction of Pdc4 expression in response to the combination of trametinib and palbociclib was also observed, suggesting that dual targeting of MEK and CDK4/6 leads to initiation of cell death signaling. It appears that this effect is independent of apoptosis, as no significant changes were observed in PARP, caspase-3, 7 or 8 in the RPPA dataset (Fig. 4D). Subsequent immunoblotting studies were carried out to confirm that COX-2 is downregulated and Pdc4 is upregulated in response to combination treatment with trametinib and palbociclib (Fig. 4E). Modulation of these biomarkers at the RNA level was addressed by carrying out RT-qPCR analysis of treated L3.6pl and UM59 cells, showing a reduction of COX-2 and an increase in Pdc4 in treated samples of both cell lines (Supplementary Fig. S4A; UM59 protein expression changes shown in Fig. S4B). Given that a decrease in COX-2 expression was the most significant change associated with activity in this study, we tested the COX-2 inhibitors celecoxib and NS-398 in the L3.6pl and UM59 models. Neither COX-2 inhibitor elicited significant anti-proliferative effects at concentrations lower than 50 μ M. Concentrations in this range have been associated with COX-independent effects and have not been achieved in humans (Supplementary Fig. S4C) (30,31). The lack of efficacy is not surprising, as significant increases in COX-2 expression in response to these inhibitors has been shown (32).

Ectopic overexpression of COX-2 lowers sensitivity to dual inhibition of MEK and CDK4/6

Based on the reduction of COX-2 expression seen when cells were co-treated with trametinib and palbociclib, experiments were undertaken to explore a direct role for COX-2 in affecting sensitivity to dual inhibition of MEK and CDK4/6. FOXM1, a transcription factor whose stability is controlled by CDK4/6 phosphorylation (33) and whose activity and cellular localization is controlled by ERK (34),

could be involved in driving this reduction in COX-2. This is possible considering FOXM1 activity has been implicated in promoting transcription of COX-2 in conjunction with Sp1 (35). The expression of FOXM1 is decreased selectively in L3.6pl cells exposed to combination treatment (Fig. 5A). Therefore, we hypothesized that combination treatment leads to synergy by decreasing expression of COX-2 through abrogation of FOXM1 activity. To test this hypothesis, a COX-2 plasmid under control of the cytomegalovirus (CMV) promoter was constructed for ectopic expression in L3.6pl cells. In this manner, removal of endogenous control of COX-2 expression would render cells unresponsive to FOXM1. After transfection, clones were selected and lysates were generated to track COX-2 expression, whereupon clone L3.6pl-C5 was found to comparatively exhibit the highest amount of COX-2 (Fig. 5B). Synergy of the parent line to the combination of trametinib and palbociclib was subsequently compared to that of the L3.6pl-C5 line and found to be significantly higher (synergy score, 7.35 vs 1.69, respectively). This finding suggests that overexpression of COX-2 by removing it from endogenous control influences the degree of synergy observed between trametinib and palbociclib. Importantly, response of the L3.6pl-C5 line to single agent treatment remained unchanged in comparison to the parent line (Supplementary Fig. S5A). However, the L3.6pl-C5 line showed a blunted shift in the concentration response curves when combining both agents at clinically relevant concentrations (1 to 10 nM trametinib and 100 nM to 1 μ M palbociclib) (Supplementary Fig. S5B). This provides evidence that, although changes in COX-2 expression may not significantly affect response to either single agent, therapeutic efficacy of the combination is reduced upon alternate transcriptional control of COX-2.

To confirm these findings *in vivo*, the parent and C5 lines were compared in tumor-bearing animals in a head to head study comparing efficacy from single agent vs combination therapy (Fig. 5C). On the last day of treatment, combination treated animals implanted with the parent line exhibited a $\Delta T/\Delta C$ value of 17%, confirming the *in vitro* synergy seen with this combination against the L3.6pl

model. In contrast, animals implanted with COX-2 overexpressing C5 tumors, exhibited a $\Delta T/\Delta C$ value of 57%. Lysates generated from tumors harvested on the last day of treatment showed decreased FOXM1 expression in both studies, consistent with earlier *in vitro* studies. Furthermore, a greater ability of combination treatment to decrease COX-2 expression was observed in the parent line in comparison to L3.6pl-C5 (Supplementary Fig. S5C). These results suggest that endogenous COX-2 expression in a model with high COX-2 expression is critical for activity and removing this factor substantially reduces *in vivo* efficacy of combination therapy in the L3.6pl model.

Knockdown of COX-2 reduces synergy to MEK and CDK4/6

Studies were designed to test the hypothesis that reduction of COX-2 expression through transcriptional control affects response to combination treatment. To explore the impact of COX-2 knockdown, L3.6pl and UM59 cells were virally transduced with COX-2 and control shRNA vectors. Despite harvesting numerous clones (>30), COX-2 was not successfully knocked down in UM59 cells, presumably due to reliance on expression for survival. In L3.6pl cells, transduction resulted in a successful knockdown of COX-2 (Fig. 5D). When these cells were evaluated for their response to combination treatment, knockdown cells showed reduced synergy in comparison to control cells (Fig.5E). This reduction in synergy is consistent with results obtained with cells previously transfected with CMV-controlled COX-2 (Fig. 5F), confirming the impact of COX-2 expression levels on therapeutic outcome in this model.

Low innate expression of COX-2 correlates with reduced benefit to combination treatment

In L3.6pl tumors, COX-2 appears to play a role in potentiating response to combination treatment. We explored the potential of COX-2 to serve as a prognostic marker of response to combination treatment across a broad panel of pancreatic cancer models. Lysates prepared from our pancreatic cell line panel were probed for expression of COX-2 (Fig. 6A). COX-2 appears as several bands, which likely

represent different potential post-translational modifications, since this protein has multiple sites for potential N-linked glycosylation, phosphorylation, and myristoylation (36). The expression levels of COX-2 in these lines was confirmed via RT-qPCR of RNA harvested from the panel (Supplementary Fig. S6A). L3.6pl and UM59 showed relatively high expression of COX-2 alongside Bxpc-3. Whereas L3.6pl and UM59 both exhibited a high degree of *in vitro* synergy to the combination of trametinib and palbociclib, a low synergy score was observed for the Bxpc-3 model. The lack of *in vitro* synergy seen here for Bxpc-3 cells is consistent with the observation that this model is exquisitely sensitive to MEK inhibition alone both *in vitro* and *in vivo* (37). Like L3.6pl, the UM59 model, which exhibited the second highest *in vitro* synergy score, showed improved therapeutic response when exposed to combination treatment, as evidenced by a 16-day tumor growth delay and $\Delta T/\Delta C$ of 5% compared to ineffective single agent therapies (Fig. 6B). Neither L3.6pl nor UM59 tumors were responsive to MEK inhibition alone. Panc-1 and Panc10.05 tumors, which exhibit low COX-2 expression (Supplementary Fig. S6B) and low *in vitro* synergy scores, showed somewhat improved response in the combination arms, as reflected by a $\Delta T/\Delta C$ value of 14% and percent regression of 21%, respectively. Most notably, one tumor-bearing mouse for each of these models showed a complete regression when treated with the combination. However, the overall improvement in response of these models to combination treatment compared to either single agent, as measured by tumor growth delay or $\Delta T/\Delta C$, was reduced compared to the L3.6pl and UM59 models, which are characterized by high COX-2 expression. Therefore, consistent with our *in vitro* data, tumors exhibiting low COX-2 expression do not appear to derive as much added benefit from the combination regimen.

Discussion

Novel therapeutic approaches for the treatment of pancreatic cancer are urgently needed due to the lack of significant improvements in patient survival over the past 40 years. Recent clinical approval

of the CDK4/6 inhibitor palbociclib provides potential new opportunities for the treatment of cancers harboring CDKN2A (p16ink4a) aberrations, which includes the majority of pancreatic cancers. Due to the high incidence of KRAS mutations in pancreatic cancer and their co-occurrence with CDKN2A inactivation, a combination therapy approach targeting MEK and CDK4/6 was evaluated here. Cell line synergy screening was carried out in both high passage and PDX models, whereupon two lines, L3.6pl and UM59, exhibited at least a twofold greater response over the median. Both models, when implanted *in vivo*, proved to be refractory to single agent treatment, while deriving substantial therapeutic benefit from the combination approach.

Importantly, co-targeting MEK and CDK4/6 was further found to potentiate cell cycle arrest in both L3.6pl and UM59 cells over that with single agent CDK4/6 inhibition. The prominent G1 arrest observed in our studies was confirmed by synergistic reductions in total levels of Cdc6, a protein critical for initiation of DNA synthesis and implicated in response to CDK4/6 modulation and RB output (26). Furthermore, reduction was seen in the expression of FOXM1, a transcription factor involved in cell cycle progression. It is a target of both ERK (34) and CDK4/6 (33), regulating cellular localization and stability, respectively.

Concurrent phosphoproteomic profiling of treated L3.6pl tumors revealed the interesting finding that COX-2 expression was downregulated in response to dual inhibition of MEK and CDK4/6. COX-2 is known for its role in mediating inflammation and promoting tumorigenesis in colorectal cancer and pancreatic cancer (38-41). While COX-2 expression can be affected by inhibition of MAPK signaling (42-44), it is unclear how inhibition of CDK4/6 synergizes with MEK to decrease expression of COX-2 in the absence of an effect by MEK inhibition. The significant reduction that we see in expression of COX-2 upon dual inhibition of MEK and CDK4/6 may ensue from reduced levels of FOXM1, as others have reported that COX-2 is in part controlled by FOXM1 activity (35,45,46). Another protein whose

expression was significantly altered by combination treatment in L3.6pl tumors was programmed cell death 4 (Pdc4), which showed significant upregulation. Studies have shown that this novel tumor suppressor negatively regulates gene expression by inhibiting Sp1/Sp3 binding at important motifs (47) and may play a role in inactivating PI3K/AKT signaling and suppressing CCND1 and CDK4 expression in NCSLC (48). This finding has potential implications for the current study in which FOXM1 is reduced by combination treatment, as other groups have shown FOXM1 cooperating with Sp1 to promote COX-2 expression (35). Pdc4 may be regulated itself by direct phosphorylation through AKT (49). It is intriguing that studies have identified Pdc4 to be in part responsible for the anticancer effects of COX-2 inhibitor NS-398 (50) in colon carcinoma. Further studies are warranted to elucidate signaling dynamics of these findings and further studies are ongoing to determine possible links. However, our studies unequivocally demonstrate that combining trametinib and palbociclib elicits a significant reduction of Ki67 staining in L3.6pl tumors, accompanied by a strong reduction in COX-2 and an increase in Pdc4, both *in vivo* and *in vitro*.

COX-2 was expressed under CMV promoter control to test the hypothesis that transcriptional control of COX-2 was responsible for the reduction in expression seen. Ectopic expression of COX-2 increased resistance to combination therapy efficacy and blunted the reduction of COX-2 seen in response to combination treatment. However, a modest but significant reduction was still seen in L3.6pl-C5 cells. This could be explained by a low level of endogenous COX-2 that continues to be expressed in these cells. Post-translational degradation mechanisms may also be in place that are being induced by combination treatment. Reports indicate caveolin-1 co-localizes with COX-2 at the plasma membrane (51,52) and participates in direct degradation of COX-2 (53). As a result, studies are warranted to investigate the role of caveolin-1 in the degradation of COX-2 in cells treated with combination therapy, as a modest increase in caveolin-1 expression was observed in the RPPA dataset in the combination arm.

Furthermore, knockdown of COX-2 in L3.6pl cells blunted the synergistic response in comparison to control cells, confirming a role for COX-2 in mediating response to co-inhibition of MEK and CDK4/6. In summary, removing COX-2 gene expression from endogenous control, either through knockdown or expression of CMV-promoter driven COX-2, reduces synergistic response. This is expected, as modulation of COX-2 expression via control of FOXM1 is ostensibly what leads to synergy when co-inhibiting MEK and CDK4/6. It is important to keep in mind that several models in our study are exceptionally sensitive to either trametinib or palbociclib alone when tested *in vitro*. Our data suggest that the usefulness of a synergy-based *in vitro* screen is biased towards models which show poor single agent activity. In particular, the L3.6pl model scored the highest in the *in vitro* combination screen and was subsequently shown to elicit no benefit from either single agent *in vivo*, while responding favorably to the combination. This is not to say that tumors exemplified by Panc-1 and Panc10.05, which produced low *in vitro* synergy scores, would not benefit from the combination *in vivo*. In fact, both of these models showed one complete regression in the combination arm. Their low synergy scores *in vitro* were partly due to their high *in vitro* sensitivity to trametinib alone. Nonetheless, trametinib monotherapy proved to be inactive in mice in all of the models tested here. This highlights the disconnect between the *in vitro* and *in vivo* settings where tumor heterogeneity, tumor microenvironment and adaptive signaling play a role.

Our goal was to identify models in which combination treatment disrupts signaling pathways that dictate their response. *In vitro* synergy screening facilitated the identification of two models, L3.6pl and UM59, that can derive substantial therapeutic benefit from dual targeting of MEK and CDK4/6. In those models, the interesting observation was made that COX-2 expression levels influence therapeutic outcome. Endogenous COX-2 expression appears to be critical for activity and its ablation substantially reduces *in vivo* efficacy of combination therapy. Interestingly, both models are adenosquamous

carcinomas of the pancreas, a highly aggressive form of pancreatic cancer reported to show strong expression of COX-2 (54-58). Further studies are warranted to better understand the prognostic significance of high expression of COX-2, a protein implicated in pancreatic cancer development (38,39,59). Our collective data suggest that such studies may help guide identification of a subpopulation of pancreatic cancer patients that could derive therapeutic benefit from co-targeting MEK and CDK4/6.

References

1. Rahib L, Smith BD, Aizenberg R, Rosenzweig AB, Fleshman JM, Matrisian LM. Projecting cancer incidence and deaths to 2030: the unexpected burden of thyroid, liver, and pancreas cancers in the United States. *Cancer research* **2014**;74(11):2913-21 doi 10.1158/0008-5472.can-14-0155.
2. Siegel RL, Miller KD, Jemal A. Cancer statistics, 2016. *CA: A Cancer Journal for Clinicians* **2016**;66(1):7-30 doi 10.3322/caac.21332.
3. Maitra A, Hruban RH. Pancreatic cancer. *Annual review of pathology* **2008**;3:157-88 doi 10.1146/annurev.pathmechdis.3.121806.154305.
4. Jaffee EM, Hruban RH, Canto M, Kern SE. Focus on pancreas cancer. *Cancer cell* **2002**;2(1):25-8 doi [http://dx.doi.org/10.1016/S1535-6108\(02\)00093-4](http://dx.doi.org/10.1016/S1535-6108(02)00093-4).
5. Liggett WH, Sidransky D. Role of the p16 tumor suppressor gene in cancer. *Journal of Clinical Oncology* **1998**;16:1197-206.
6. Cox AD, Fesik SW, Kimmelman AC, Luo J, Der CJ. Drugging the undruggable RAS: Mission Possible? *Nature Reviews Drug Discovery* **2014**;13:828 doi 10.1038/nrd4389 <https://www.nature.com/articles/nrd4389#supplementary-information>.
7. Serrano M, Lin AW, McCurrach ME, Beach D, Lowe SW. Oncogenic ras provokes premature cell senescence associated with accumulation of p53 and p16INK4a. *Cell* **1997**;88(5):593-602.
8. Wee S, Jagani Z, Xiang KX, Loo A, Dorsch M, Yao YM, *et al.* PI3K pathway activation mediates resistance to MEK inhibitors in KRAS mutant cancers. *Cancer research* **2009**;69(10):4286-93 doi 10.1158/0008-5472.can-08-4765.
9. Little AS, Balmano K, Sale MJ, Newman S, Dry JR, Hampson M, *et al.* Amplification of the Driving Oncogene, KRAS or BRAF, Underpins Acquired Resistance to MEK1/2 Inhibitors in Colorectal Cancer Cells. 2011. ra17-ra p.
10. Poulidakos PI, Solit DB. Resistance to MEK Inhibitors: Should We Co-Target Upstream? 2011. pe16-pe p.
11. Turke AB, Song Y, Costa C, Cook R, Arteaga CL, Asara JM, *et al.* MEK inhibition leads to PI3K/AKT activation by relieving a negative feedback on ERBB receptors. *Cancer research* **2012**;72(13):3228-37 doi 10.1158/0008-5472.CAN-11-3747.
12. Blagosklonny MV, Pardee AB. The Restriction Point of the Cell Cycle. *Cell cycle (Georgetown, Tex)* **2002**;1(2):102-9 doi 10.4161/cc.1.2.108.
13. Puyol M, Martín A, Dubus P, Mulero F, Pizcueta P, Khan G, *et al.* A Synthetic Lethal Interaction between K-Ras Oncogenes and Cdk4 Unveils a Therapeutic Strategy for Non-small Cell Lung Carcinoma. *Cancer cell*;18(1):63-73 doi 10.1016/j.ccr.2010.05.025.
14. Kwong LN, Costello JC, Liu H, Jiang S, Helms TL, Langsdorf AE, *et al.* Oncogenic NRAS signaling differentially regulates survival and proliferation in melanoma. *Nature medicine* **2012**;18(10):1503-10 doi 10.1038/nm.2941.
15. Ziemke EK, Dosch JS, Maust JD, Shettigar A, Sen A, Welling TH, *et al.* Sensitivity of KRAS Mutant Colorectal Cancers to Combination Therapy that Co-Targets MEK and CDK4/6. *Clinical cancer research : an official journal of the American Association for Cancer Research* **2015** doi 10.1158/1078-0432.ccr-15-0829.
16. Lee MS, Helms TL, Feng N, Gay J, Chang QE, Tian F, *et al.* Efficacy of the combination of MEK and CDK4/6 inhibitors in vitro and in vivo in KRAS mutant colorectal cancer models. *Oncotarget* **2016**;7(26):39595-608 doi 10.18632/oncotarget.9153.
17. Bardeesy N, Aguirre AJ, Chu GC, Cheng KH, Lopez LV, Hezel AF, *et al.* Both p16(Ink4a) and the p19(Arf)-p53 pathway constrain progression of pancreatic adenocarcinoma in the mouse. *Proceedings of the National Academy of Sciences of the United States of America* **2006**;103(15):5947-52 doi 10.1073/pnas.0601273103.
18. Calbo J, Marotta M, Cascallo M, Roig JM, Gelpi JL, Fueyo J, *et al.* Adenovirus-mediated wt-p16 reintroduction induces cell cycle arrest or apoptosis in pancreatic cancer. *Cancer gene therapy* **2001**;8(10):740-50 doi 10.1038/sj.cgt.7700374.
19. Franco J, Balaji U, Freinkman E, Witkiewicz AK, Knudsen ES. Metabolic Reprogramming of Pancreatic Cancer Mediated by CDK4/6 Inhibition Elicits Unique Vulnerabilities. *Cell reports* **2016**;14(5):979-90 doi 10.1016/j.celrep.2015.12.094.
20. Franco J, Witkiewicz AK, Knudsen ES. CDK4/6 inhibitors have potent activity in combination with pathway selective therapeutic agents in models of pancreatic cancer. *Oncotarget* **2014**.
21. Tuominen VJ, Ruotoistenmäki S, Viitanen A, Jumppanen M, Isola J. ImmunoRatio: a publicly available web application for quantitative image analysis of estrogen receptor (ER), progesterone receptor (PR), and Ki-67. *Breast Cancer Research* **2010**;12(4):1-12 doi 10.1186/bcr2615.

22. Tao Z, Le Blanc JM, Wang C, Zhan T, Zhuang H, Wang P, *et al.* Coadministration of Trametinib and Palbociclib Radiosensitizes KRAS-Mutant Non-Small Cell Lung Cancers In Vitro and In Vivo. *Clinical cancer research : an official journal of the American Association for Cancer Research* **2016**;22(1):122-33 doi 10.1158/1078-0432.ccr-15-0589.
23. Cheng Y, Tian H. Current Development Status of MEK Inhibitors. *Molecules* **2017**;22(10):1551.
24. Duso BA, Trapani D, Viale G, Criscitiello C, D'Amico P, Belli C, *et al.* Clinical efficacy of ribociclib as a first-line therapy for HR-positive, advanced breast cancer. *Expert opinion on pharmacotherapy* **2018**;19(3):299-305 doi 10.1080/14656566.2018.1429407.
25. Liu J, Smith CL, DeRyckere D, DeAngelis K, Martin GS, Berger JM. Structure and function of Cdc6/Cdc18: implications for origin recognition and checkpoint control. *Mol Cell* **2000**;6(3):637-48.
26. Braden WA, McClendon AK, Knudsen ES. Cyclin-dependent kinase 4/6 activity is a critical determinant of pre-replication complex assembly. *Oncogene* **2008**;27(56):7083-93 doi 10.1038/onc.2008.319.
27. Lavoie JN, L'Allemain G, Brunet A, Müller R, Pouysségur J. Cyclin D1 Expression Is Regulated Positively by the p42/p44MAPK and Negatively by the p38/HOGMAPK Pathway. *Journal of Biological Chemistry* **1996**;271:20608-16 doi 10.1074/jbc.271.34.20608.
28. Ray A, James MK, Larochele S, Fisher RP, Blain SW. p27(Kip1) Inhibits Cyclin D-Cyclin-Dependent Kinase 4 by Two Independent Modes. *Molecular and cellular biology* **2009**;29(4):986-99 doi 10.1128/mcb.00898-08.
29. Qin G, Xu F, Qin T, Zheng Q, Shi D, Xia W, *et al.* Palbociclib inhibits epithelial-mesenchymal transition and metastasis in breast cancer via c-Jun/COX-2 signaling pathway. *Oncotarget* **2015**;6(39):41794-808 doi 10.18632/oncotarget.5993.
30. Hawk ET, Viner JL, Dannenberg A, DuBois RN. COX-2 in Cancer—A Player That's Defining the Rules. *JNCI: Journal of the National Cancer Institute* **2002**;94(8):545-6 doi 10.1093/jnci/94.8.545.
31. Davies NM, McLachlan AJ, Day RO, Williams KM. Clinical Pharmacokinetics and Pharmacodynamics of Celecoxib. *Clinical Pharmacokinetics* **2000**;38(3):225-42 doi 10.2165/00003088-200038030-00003.
32. Ferguson S, Hebert RL, Laneuville O. NS-398 upregulates constitutive cyclooxygenase-2 expression in the M-1 cortical collecting duct cell line. *Journal of the American Society of Nephrology : JASN* **1999**;10(11):2261-71.
33. Anders L, Ke N, Hydrbring P, Choi YJ, Widlund HR, Chick JM, *et al.* A systematic screen for CDK4/6 substrates links FOXM1 phosphorylation to senescence suppression in cancer cells. *Cancer cell* **2011**;20(5):620-34 doi 10.1016/j.ccr.2011.10.001.
34. Ma RY, Tong TH, Cheung AM, Tsang AC, Leung WY, Yao KM. Raf/MEK/MAPK signaling stimulates the nuclear translocation and transactivating activity of FOXM1c. *Journal of cell science* **2005**;118(Pt 4):795-806 doi 10.1242/jcs.01657.
35. Xu K, Shu H-KG. The FOXM1 transcription factor interacts with Sp1 to mediate EGF-dependent COX-2 expression in human glioma cells. *Molecular cancer research : MCR* **2013**;11(8):875-86 doi 10.1158/1541-7786.MCR-12-0706.
36. Wennogle LP, Liang H, Quintavalla JC, Bowen BR, Wasvary J, Miller DB, *et al.* Comparison of recombinant cyclooxygenase-2 to native isoforms: aspirin labeling of the active site. *FEBS Lett* **1995**;371(3):315-20.
37. Allen LF, Sebolt-Leopold J, Meyer MB. CI-1040 (PD184352), a targeted signal transduction inhibitor of MEK (MAPKK). *Seminars in oncology* **2003**;30(5 Suppl 16):105-16.
38. Hill R, Li Y, Tran LM, Dry S, Calvopina JH, Garcia A, *et al.* Cell intrinsic role of COX-2 in pancreatic cancer development. *Molecular cancer therapeutics* **2012**;11(10):2127-37 doi 10.1158/1535-7163.mct-12-0342.
39. Yip-Schneider MT, Barnard DS, Billings SD, Cheng L, Heilman DK, Lin A, *et al.* Cyclooxygenase-2 expression in human pancreatic adenocarcinomas. *Carcinogenesis* **2000**;21(2):139-46 doi 10.1093/carcin/21.2.139.
40. Ogino S, Kirkner GJ, Nosho K, Irahara N, Kure S, Shima K, *et al.* Cyclooxygenase-2 expression is an independent predictor of poor prognosis in colon cancer. *Clinical cancer research : an official journal of the American Association for Cancer Research* **2008**;14(24):8221-7 doi 10.1158/1078-0432.ccr-08-1841.
41. Eberhart CE, Coffey RJ, Radhika A, Giardiello FM, Ferrenbach S, DuBois RN. Up-regulation of cyclooxygenase 2 gene expression in human colorectal adenomas and adenocarcinomas. *Gastroenterology* **1994**;107(4):1183-8.
42. Elder DJ, Halton DE, Playle LC, Paraskeva C. The MEK/ERK pathway mediates COX-2-selective NSAID-induced apoptosis and induced COX-2 protein expression in colorectal carcinoma cells. *International journal of cancer Journal international du cancer* **2002**;99(3):323-7 doi 10.1002/ijc.10330.
43. Schmidt CM, Wang Y, Wiesenauer C. Novel combination of cyclooxygenase-2 and MEK inhibitors in human hepatocellular carcinoma provides a synergistic increase in apoptosis. *Journal of gastrointestinal surgery : official journal of the Society for Surgery of the Alimentary Tract* **2003**;7(8):1024-33.
44. Huang F, Cao J, Liu Q, Zou Y, Li H, Yin T. MAPK/ERK signal pathway involved expression of COX-2 and VEGF by IL-1 β induced in human endometriosis stromal cells in vitro. *International Journal of Clinical and Experimental Pathology* **2013**;6(10):2129-36.

45. Ahmed M, Hussain AR, Siraj AK, Uddin S, Al-Sanea N, Al-Dayel F, *et al.* Co-targeting of Cyclooxygenase-2 and FoxM1 is a viable strategy in inducing anticancer effects in colorectal cancer cells. *Molecular cancer* **2015**;14:131 doi 10.1186/s12943-015-0406-1.
46. Xu K, Shu HK. Transcription factor interactions mediate EGF-dependent COX-2 expression. *Mol Cancer Res* **2013**;11(8):875-86 doi 10.1158/1541-7786.mcr-12-0706.
47. Leupold JH, Yang HS, Colburn NH, Asangani I, Post S, Allgayer H. Tumor suppressor Pcdcd4 inhibits invasion/intravasation and regulates urokinase receptor (u-PAR) gene expression via Sp-transcription factors. *Oncogene* **2007**;26(31):4550-62 doi 10.1038/sj.onc.1210234.
48. Zhen Y, Li D, Li W, Yao W, Wu A, Huang J, *et al.* Reduced PDCD4 Expression Promotes Cell Growth Through PI3K/Akt Signaling in Non-Small Cell Lung Cancer. *Oncology research* **2016**;23(1-2):61-8 doi 10.3727/096504015x14478843952861.
49. Palamarchuk A, Efanov A, Maximov V, Aqeilan RI, Croce CM, Pekarsky Y. Akt phosphorylates and regulates Pcdcd4 tumor suppressor protein. *Cancer research* **2005**;65(24):11282-6 doi 10.1158/0008-5472.can-05-3469.
50. Zhang Z, DuBois RN. Detection of differentially expressed genes in human colon carcinoma cells treated with a selective COX-2 inhibitor. *Oncogene* **2001**;20(33):4450-6 doi 10.1038/sj.onc.1204588.
51. Liou JY, Deng WG, Gilroy DW, Shyue SK, Wu KK. Colocalization and interaction of cyclooxygenase-2 with caveolin-1 in human fibroblasts. *The Journal of biological chemistry* **2001**;276(37):34975-82 doi 10.1074/jbc.M105946200.
52. Perrone G, Zagami M, Altomare V, Battista C, Morini S, Rabitti C. COX-2 localization within plasma membrane caveolae-like structures in human lobular intraepithelial neoplasia of the breast. *Virchows Archiv : an international journal of pathology* **2007**;451(6):1039-45 doi 10.1007/s00428-007-0506-4.
53. Chen SF, Liou JY, Huang TY, Lin YS, Yeh AL, Tam K, *et al.* Caveolin-1 facilitates cyclooxygenase-2 protein degradation. *Journal of cellular biochemistry* **2010**;109(2):356-62 doi 10.1002/jcb.22407.
54. Brody JR, Costantino CL, Potoczek M, Cozzitorto J, McCue P, Yeo CJ, *et al.* Adenosquamous carcinoma of the pancreas harbors KRAS2, DPC4 and TP53 molecular alterations similar to pancreatic ductal adenocarcinoma. *Modern pathology : an official journal of the United States and Canadian Academy of Pathology, Inc* **2009**;22(5):651-9 doi 10.1038/modpathol.2009.15.
55. Katz MH, Taylor TH, Al-Refaie WB, Hanna MH, Imagawa DK, Anton-Culver H, *et al.* Adenosquamous versus adenocarcinoma of the pancreas: a population-based outcomes analysis. *Journal of gastrointestinal surgery : official journal of the Society for Surgery of the Alimentary Tract* **2011**;15(1):165-74 doi 10.1007/s11605-010-1378-5.
56. Meitner PA, Kajiji SM, LaPosta-Frazier N, Bogaars HA, Jolly GA, Dexter DL, *et al.* "COLO 357," a human pancreatic adenosquamous carcinoma: growth in artificial capillary culture and in nude mice. *Cancer research* **1983**;43(12 Pt 1):5978-85.
57. Wang L, Tsutsumi S, Kawaguchi T, Nagasaki K, Tatsuno K, Yamamoto S, *et al.* Whole-exome sequencing of human pancreatic cancers and characterization of genomic instability caused by MLH1 haploinsufficiency and complete deficiency. *Genome Research* **2012**;22(2):208-19 doi 10.1101/gr.123109.111.
58. Okami J, Yamamoto H, Fujiwara Y, Tsujie M, Kondo M, Noura S, *et al.* Overexpression of cyclooxygenase-2 in carcinoma of the pancreas. *Clinical cancer research : an official journal of the American Association for Cancer Research* **1999**;5(8):2018-24.
59. Cascinu S, Scartozzi M, Carbonari G, Pierantoni C, Verdecchia L, Mariani C, *et al.* COX-2 and NF-KB overexpression is common in pancreatic cancer but does not predict for COX-2 inhibitors activity in combination with gemcitabine and oxaliplatin. *American journal of clinical oncology* **2007**;30(5):526-30 doi 10.1097/COC.0b013e318054675c.
60. Forbes SA, Tang G, Bindal N, Bamford S, Dawson E, Cole C, *et al.* COSMIC (the Catalogue of Somatic Mutations in Cancer): a resource to investigate acquired mutations in human cancer. *Nucleic acids research* **2010**;38(Database issue):D652-7 doi 10.1093/nar/gkp995.
61. Kern SE. 2018-06-21. The Genetics of Pancreatic Cancer. <<http://pathology.jhu.edu/pancreas/geneticsweb/Profiles.htm>>. Accessed 2018 2018-06-21.
62. Soucek JJ, Baine MJ, Lin C, Rachagani S, Gupta S, Kaur S, *et al.* Unbiased analysis of pancreatic cancer radiation resistance reveals cholesterol biosynthesis as a novel target for radiosensitisation. *Br J Cancer* **2014**;111(6):1139-49 doi 10.1038/bjc.2014.385.
63. Yarbrough WG, Buckmire RA, Bessho M, Liu ET. Biologic and biochemical analyses of p16(INK4a) mutations from primary tumors. *Journal of the National Cancer Institute* **1999**;91(18):1569-74.

Figure 1: Dual inhibition of MEK and CDK4/6 shows synergy in pancreatic cancer cell lines. (A)

Evaluation of synergy in 20 pancreatic cancer cell lines identifies a range of response to combination treatment. Synergy scores represent a consolidated quantitative measure of proliferation in response to 25 unique combinations of trametinib and palbociclib concentrations after being treated for 5 days, as calculated by Chalice software. Scores represent the mean of 2-4 biological replicates +/- standard error of the mean (SEM). Genetic alterations for CDKN2A and KRAS are shown for each line. (B) Synergy scores were median centered and expressed as the \log_2 difference from the median with a 95% confidence interval. (C) Synergy plots generated by Combenefit showing the interaction between trametinib and palbociclib are shown for the highest and lowest responder models (n=4, technical replicates), alongside the primary data from the same experiment showing the shift in the trametinib concentration response curve upon addition of 1 μ M palbociclib for each line (n = 4, +/- SEM). Data shown are representative and consistent with replicate experiments.

¹ATCC database, ²COSMIC (60), ³Genetics of Pancreatic Cancer (61), ⁴(62)

*p.V487_P492>A, HD = homozygous deletion, methylated = promoter methylation, fs = frameshift mutation. p16 mutation D84G confers loss of function (63). Inactivation of CDKN2A was determined via immunoblot (no detectable protein).

Figure 2: Cell cycle effects of CDK4/6 inhibition are enhanced by MEK inhibition in L3.6pl and

UM59 cells. (A) Cell cycle analysis shows evidence for G1 arrest in cells treated with palbociclib and trametinib for 48 hours. (B) Cells were treated with 10 nM trametinib or 1 μ M palbociclib, alone or in combination for the indicated time period.

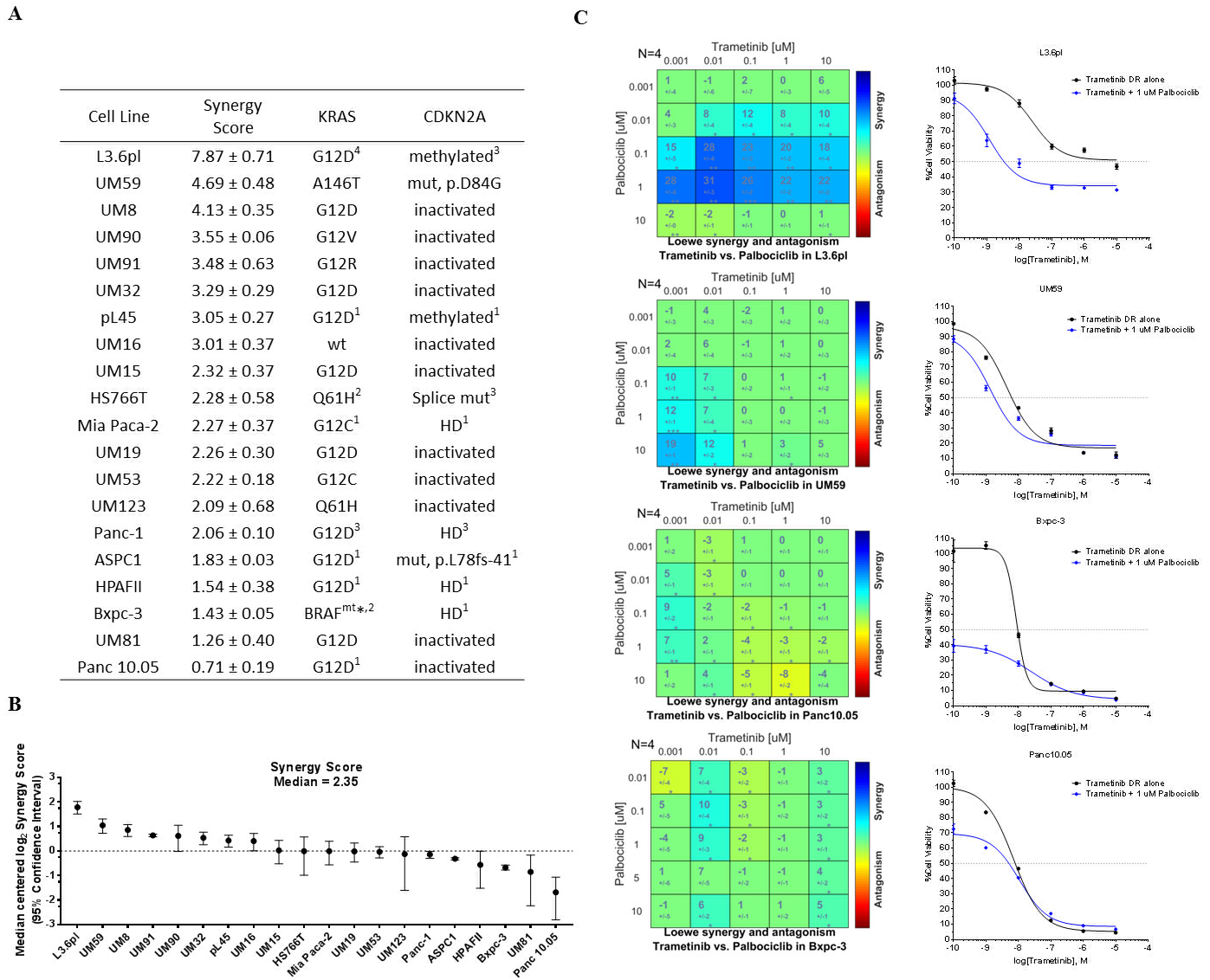
Figure 3: Single agent treatment with trametinib and palbociclib inhibits phosphorylation of Rb and ERK. (A) Concentration response of the effects of trametinib and palbociclib on Rb, ERK and cyclin D1 after 5 days of treatment. (B) Concentration response curves showing effects of trametinib and palbociclib on the proliferation of two cell lines with high synergy score (L3.6pl & UM59) and two with the low synergy score (Panc10.05 & Bxpc-3). Data are representative of multiple experiments and expressed as mean +/- SEM, n = 4 per point, treatment duration of 5 days.

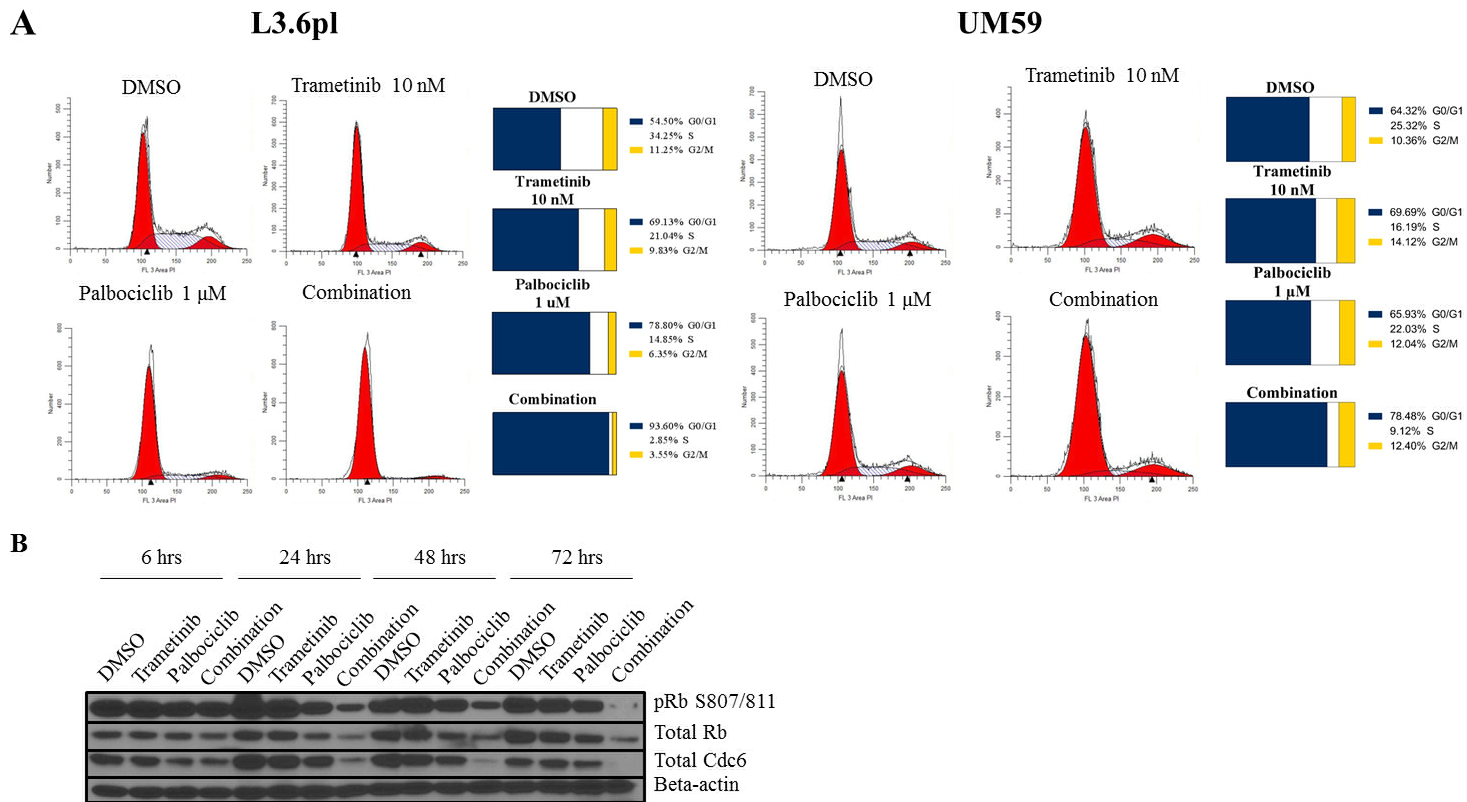
Figure 4: Combination treatment is efficacious *in vivo* and correlates with decreased COX-2 expression. (A) L3.6pl cells were implanted subcutaneously and treatment was administered once daily via oral gavage for 10 days (shaded region) or until the group mean reached 1000 mm³ (n = 5 per group). Tumors were harvested from a separate cohort on Day 7 (dotted line) for pharmacodynamic analysis. (B and C) Immunohistochemistry for Ki67 was performed and quantified (Immunoratio) in Figure B as a ratio between Ki67 stained nuclei and total nuclear area, while C shows representative images of treated tumors. (D) Heatmap generated from RPPA analysis of tumor lysates showing changes in protein expression. (E) RPPA results were verified via immunoblotting analysis for COX-2 and Pcdcd4 expression. ** indicates p < 0.005, *** p < 0.0005, **** p < 0.0001, in comparison to combination arm.

Figure 5: COX-2 expression is implicated in sensitivity to co-targeting of MEK and CDK4/6. (A) Immunoblotting analysis of FOXM1 expression in L3.6pl cells harvested after a 5-day treatment with the indicated conditions. (B) Six clones expressing the CMV driven hCOX-2 construct were compared to the parent L3.6pl cell line for expression of COX-2. (C) A clone shown to express constitutively high levels of COX-2 (C5) was compared to the parent line in a head-to-head *in vivo* study (n = 5 per

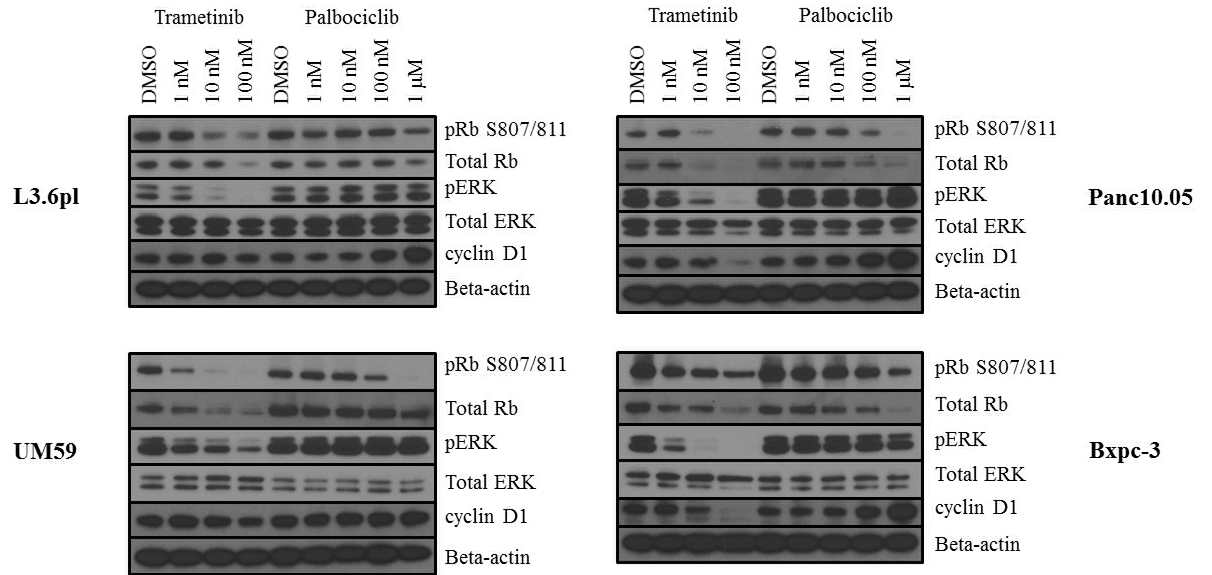
treatment condition, treatment period is shaded). Tumor burden was monitored during treatment and T/C values are shown for all treatment conditions. (D) Lysates were collected multiple times from L3.6pl cells expressing either a control shRNA plasmid or COX-2 shRNA to confirm COX-2 knockdown. (E) Combobenefit graphs showing a reduced synergistic response of L3.6pl cells expressing COX-2 shRNA. (F) This chart lists the mean synergy scores +/- SEM of each cell line derived from L3.6pl to test the role of COX-2. ns indicates $p > 0.05$, * $p < 0.05$, ** $p < 0.005$, *** $p < 0.0005$, **** $p < 0.0001$, in comparison to combination arm.

Figure 6: High expression of COX-2 correlates with greater relative benefit in the *in vitro* synergy screen and in tumor-bearing animals. (A) Expression of COX-2 in the panel of pancreatic cancer cell lines tested in the synergy screen. (B) *In vivo* studies were conducted in mice subcutaneously implanted with either UM59 (n = 4 per group), Panc-1 (n = 3 per group) or Panc10.05 (n = 5 per group) cells. Drugs were administered once daily via oral gavage for 10 days (shaded region) once tumors reached roughly 150-200 mm³. The percent treatment/control (%T/C) and $\Delta T/\Delta C$ on the last day of treatment as well as tumor growth delay (calculated at 750 mm³ for UM59 and Panc-1, and 700 mm³ for Panc10.05) are shown for each *in vivo* experiment. * indicates $p < 0.05$, ** $p < 0.005$, in comparison to combination arm on last day of treatment. Panc10.05 p values indicated on lower right of graph and were calculated based on T/C values, as a negative $\Delta T/\Delta C$ cannot be calculated accurately. If no p values were indicated, differences are not statistically significant.





A



B

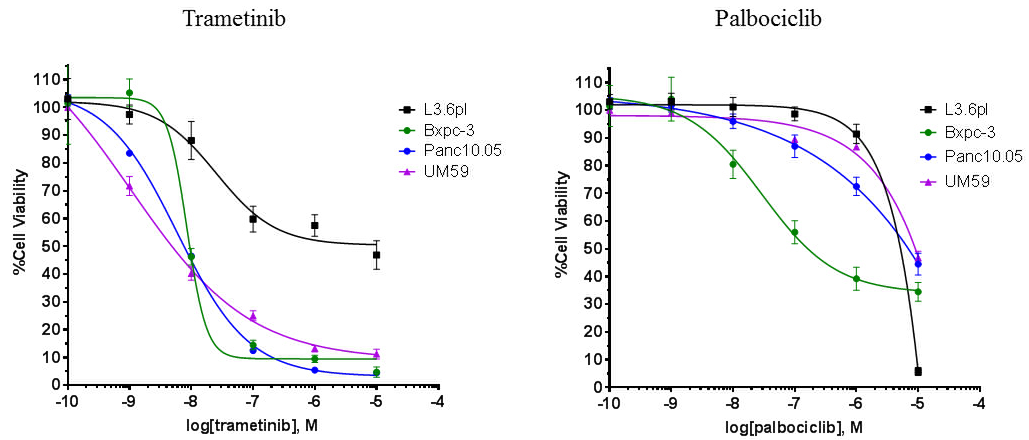
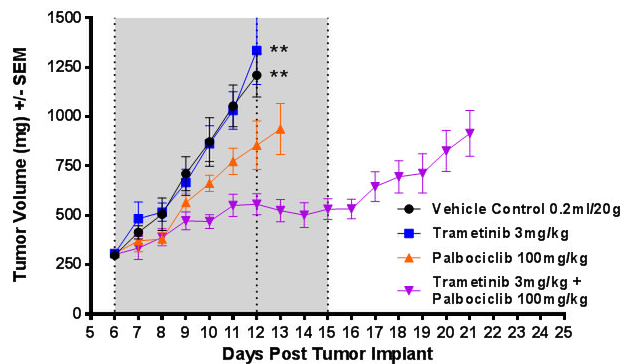
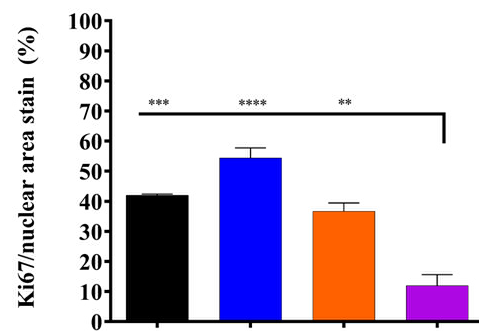


Figure 4

A

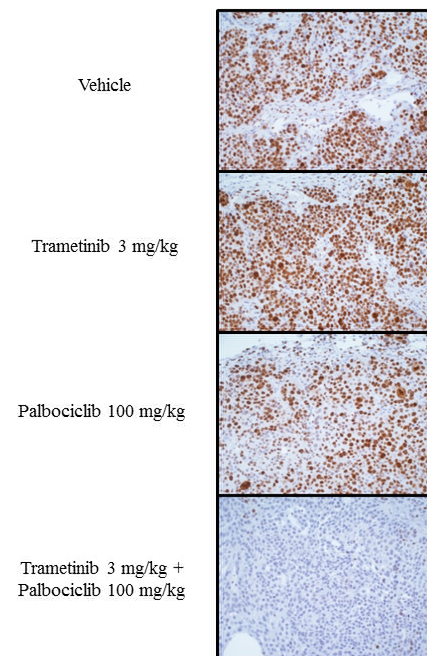


B

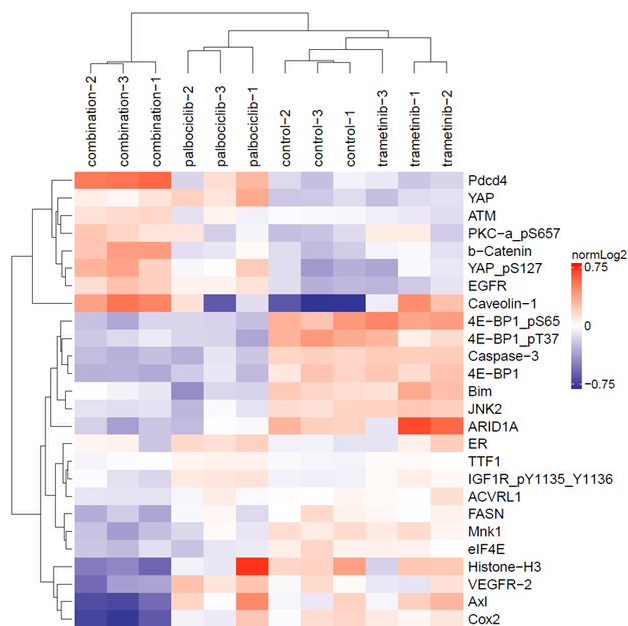


Treatment Group	Tumor Growth Delay	$\Delta T/\Delta C$ (Day 12)
Trametinib 3 mg/kg	0 days	97 ± 14 %
Palbociclib 100 mg/kg	1 days	62 ± 8 %
Trametinib 3 mg/kg + Palbociclib 100 mg/kg	10 days	29 ± 5 %

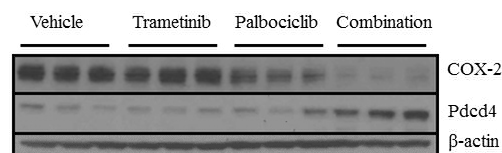
C



D



E



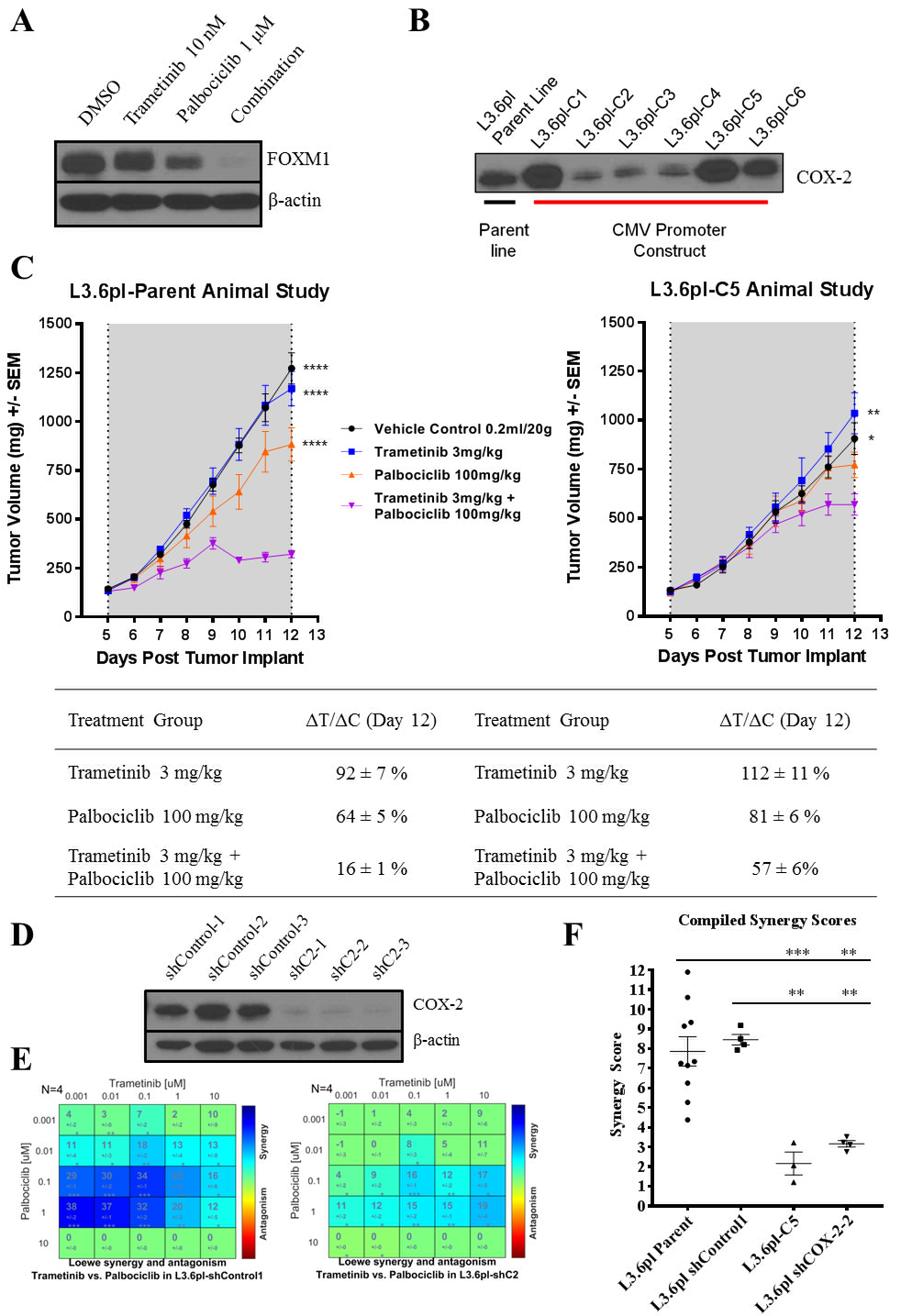
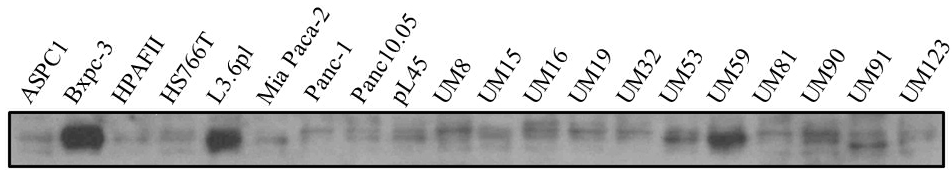
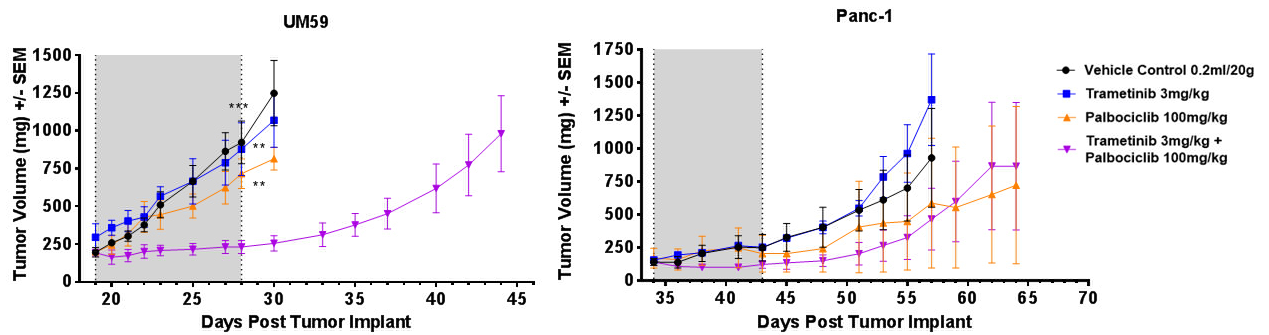


Figure 6

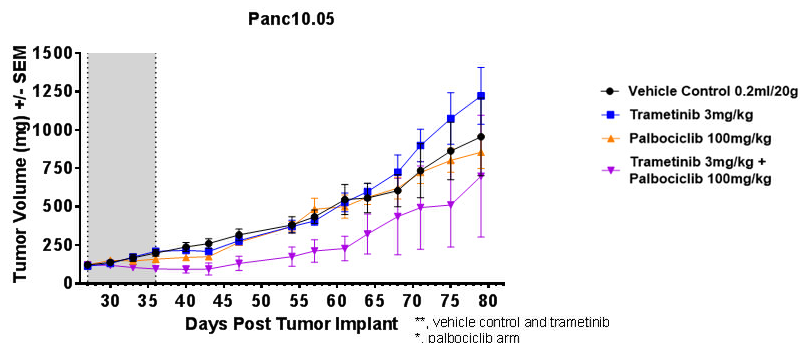
A



B



Treatment Group	Tumor Growth Delay	$\Delta T/\Delta C$ (Day 28)	Treatment Group	Tumor Growth Delay	$\Delta T/\Delta C$ (Day 43)
Trametinib 3 mg/kg	1 days	81 ± 12 %	Trametinib 3 mg/kg	0 days	54 ± 14 %
Palbociclib 100 mg/kg	3 days	71 ± 10 %	Palbociclib 100 mg/kg	9 days	41 ± 46 %
Trametinib 3 mg/kg + Palbociclib 100 mg/kg	16 days	5 ± 4 %	Trametinib 3 mg/kg + Palbociclib 100 mg/kg	5 days	14 ± 12 %



Treatment Group	Tumor Growth Delay	$\Delta T/\Delta C$ (Day 36)	Percent Regression
Trametinib 3 mg/kg	0 days	126 ± 20 %	
Palbociclib 100 mg/kg	0 days	49 ± 24 %	
Trametinib 3 mg/kg + Palbociclib 100 mg/kg	9 days	N/A	21%

Molecular Cancer Therapeutics

Cyclooxygenase-2 Influences Response to Co-Targeting of MEK and CDK4/6 in a Subpopulation of Pancreatic Cancers

Joel D Maust, Christy L Frankowski-McGregor, Armand Bankhead, et al.

Mol Cancer Ther Published OnlineFirst September 25, 2018.

Updated version	Access the most recent version of this article at: doi: 10.1158/1535-7163.MCT-18-0082
Supplementary Material	Access the most recent supplemental material at: http://mct.aacrjournals.org/content/suppl/2018/09/25/1535-7163.MCT-18-0082.DC1
Author Manuscript	Author manuscripts have been peer reviewed and accepted for publication but have not yet been edited.

E-mail alerts [Sign up to receive free email-alerts](#) related to this article or journal.

Reprints and Subscriptions To order reprints of this article or to subscribe to the journal, contact the AACR Publications Department at pubs@aacr.org.

Permissions To request permission to re-use all or part of this article, use this link <http://mct.aacrjournals.org/content/early/2018/09/25/1535-7163.MCT-18-0082>. Click on "Request Permissions" which will take you to the Copyright Clearance Center's (CCC) Rightslink site.